Contents lists available at ScienceDirect

Applied Surface Science

Full Length Article

Nanostructured interfaces with site-specific bioreceptors for immunosensing

Telmo O. Paiva [a,1], Inês Almeida [a,1], Joaquim T. Marquês [a], Wei Liu [b,c], Yu Niu [b], Gang Jin [b,d,**], Ana S. Viana [a,*]

[a] Centro de Química e Bioquímica, Faculdade de Ciências, Universidade de Lisboa, Campo Grande, Edifício C8, 1749-016 Lisboa, Portugal
[b] NML, Institute of Mechanics, Chinese Academy of Sciences, Beijing, 100190, China
[c] Institute of Microelectronics, Tsinghua University, Beijing 100084, China
[d] School of Engineering Science, University of Chinese Academy of Sciences, Beijing 100049, China

ABSTRACT

In this work, we propose a simple and effective approach to build nanostructured immunosensor platforms. The one-step strategy relies on i) the *in situ* formation of dithiocarbamates from the reaction between carbon disulfide and amine groups, present on protein A, ii) their attachment to gold nanoparticles (AuNPs), and iii) the linkage of the modified AuNPs to the electrode surface, which depends on the strong interaction between gold substrates and sulfur moieties. AuNPs and protein A are used to increase the surface coverage of Immunoglobulin G (IgG) and promote the oriented immobilization of the antibodies on the immunosensing interface. The modified gold surfaces with biomolecules were thoroughly characterized by a combination of techniques: UV–vis spectrophotometry, conventional ellipsometry and atomic force microscopy. The immunosensor performance was assessed in real-time, by surface plasmon resonance and by the highly sensitive total internal reflection imaging ellipsometry, through the specific biorecognition between anti-IgG and the immobilized IgG molecules. We demonstrate that the presence of AuNPs improves the sensitivity of the anti-IgG specific detection, whereas the presence of co-adsorbed CS_2 is responsible for blocking the undesired protein nonspecific adsorption to the gold substrate. Overall, we report a simple and innovative one-step method, to chemically modify gold surfaces with protein A and AuNPs, able to specifically detect antigen/antibody interactions with capability of preventing protein nonspecific adsorption.

© 2017 Elsevier B.V. All rights reserved.

1. Introduction

Gold surface modification has been a useful and highly promising approach for biosensing purposes. One of the most popular strategies of surface modification are the self-assembled monolayers (SAM), which form spontaneously, through the adsorption of molecular compounds to solid surfaces [1]. Using alkanethiol molecules, highly organized and stable platforms with reproducibility and easy preparation can be developed [2–4]. Moreover, alkanethiol molecules containing terminal functional groups, such as carboxylic acid moieties, are suit-

able to covalently immobilize proteins [5–8]. However, this method requires the incorporation of an activation step, usually performed with *N*-hydroxysuccinimide (NHS) and 1-ethyl-3-(3-dimethylaminopropyl) carbodiimide (EDC), to attach the protein to the SAM [8–10]. An approach using the *in situ* formation of dithiocarbamates (DTC) to, in only one-step, immobilize compounds with amine groups to gold surfaces has been developed as an efficient alternative [11–13]. Briefly, carbon disulfide spontaneously reacts with amine groups to form DTC through the immersion of gold substrates in a solution containing CS_2 and the compound to immobilize, at room temperature [11,14,15], without the need of adding several modification and activation steps. DTC have a resonant bidentate structure along N-C-S_2 and establish strong linkages to gold substrates [16]. This methodology has been used to immobilize a wide range of molecules and biocompounds [13,17–21] and, importantly, to prepare immunosensor interfaces for the detection of biological molecules relying on the specific antibody-antigen reaction. Furthermore, the ability to prevent protein nonspecific

* Corresponding author at: Centro de Química e Bioquímica, Faculdade de Ciências, Universidade de Lisboa, Campo Grande, Ed. C8, 1749-016 Lisboa, Portugal.
** Corresponding author at: NML, Institute of Mechanics, Chinese Academy of Sciences, Beijing, 100190, China.
E-mail addresses: gajin@imech.ac.cn (G. Jin), anaviana@fc.ul.pt (A.S. Viana).
[1] These authors contributed equally to the work.

adsorption to the biorecognition surfaces has been also demonstrated [12].

Beyond the high stability, biocompatibility and versatility, the detection limit is the major concern regarding immunosensors development. It has to be high enough to allow the detection of small target molecules in clinical or environmental samples, usually present in trace amounts. Since gold nanoparticles (AuNPs) display high surface area with good biocompatibility and singular optical properties [19,22,23], they present a possible approach to enhance the immunosensors efficiency and sensitivity [24–26]. The principle behind the signal enhancement in the optical immunosensors using the surface plasmon resonance (SPR) effect, relies on the shift of the plasmon resonance angle of the gold thin layer, due to the electronic coupling interaction with the nanoparticles localized surface plasmon wave [27–29]. Furthermore, by using AuNPs directly adsorbed on gold surfaces, a proper orientation and distribution of the antibodies can also be achieved. These phenomena, isolated or combined, enable the appearance of large changes in the SPR signal, increasing the detection sensitivity and therefore, decreasing the minimum of detectable molecules [30]. In fact, there are many studies reporting the functionalization of AuNPs with specific antibodies towards the detection of cancer biomarkers in a sandwich type immunosensor (e.g. prostate specific antigen) [25,26,31,32].

Aiming the preparation of biosensing platforms, we have developed innovative self-assembly procedures using carbon disulfide for the robust immobilization of protein A [12], enzymes conjugated with AuNPs [34] or iron oxide nanoparticles [33,21], on flat gold surfaces. Hereby, we combine these simple chemical approaches to prepare sensitive three-dimensional immunosensing platforms, using the *in situ* DTC reaction between CS_2 and amine groups of protein A, in the presence of AuNPs. Fig. 1 shows a schematic representation of the one-pot methodology used in this work for surface modification, with proposed adsorbates that are prone to interact with gold: nanoassemblies, CS_2 and dithiocarbamates. Protein A/AuNPs bioconjugates allow the immobilization of a large amount of immunoglobulin G (IgG) molecules, in an oriented assemble, through the specific interaction with the Fc portion, which enables the recognition by anti-IgG molecules via Fab portions [31,35]. This novel nanostructured interface developed for IgG/anti-IgG is versatile and can be easily adapted to detect any target molecules of interest through the use of appropriate antibodies, including sandwich-based architectures. This pair of antibodies, used as a proof of concept, mimics the natural and high specific antigen/antibody interaction. A combination of techniques, including UV–vis spectrophotometry, atomic force microscopy (AFM), SPR, conventional ellipsometry and total internal reflection imaging ellipsometry (TIRIE) was employed to characterize the properties and the performance of this newly created platform.

2. Experimental

2.1. Chemicals

Carbon disulfide, protein A from *Staphylococcus aureus* and the antibodies for immunosensing, human IgG and polyclonal anti-human IgG (H + L) secondary antibody from goat, and casein-based blocking buffer (BB) were obtained from Sigma-Aldrich and used without further purification. Phosphate buffer saline (PBS, 0.01 M phosphate buffer, 0.0027 M potassium chloride and 0.137 M sodium chloride), pH 7.4, obtained from Sigma-Aldrich, with (PBST) or without 0.05% (v/v) of Tween20, prepared with ultrapure Milli-Q water (18.2 MΩ cm) was used for the preparation of protein solutions and as a washing solution in SPR and TIRIE experiments.

2.2. Preparation of gold surfaces

Two types of gold substrates have been used in this work. For SPR experiments, polycrystalline gold (50 nm) coated glass slides, with a uniform granular morphology, purchased from Analytical μ-Systems. Prior to use, the slides were rinsed with water and ethanol and cleaned in a UV chamber for 45 min. For AFM and ellipsometry, thin layer gold surfaces, manufactured by Arrandee, consisting of a thin film (200 nm) on borosilicate glass (1.1 × 1.1 cm^2) with a chromium undercoat (2–4 nm) were used. The surfaces were firstly flame-annealed to acquire a preferential (111) orientation [13] and cleaned in piranha solution ($H_2SO_4/H_2O_2 = 3:1$, v/v) and in a UV chamber for 45 min, as described elsewhere [12,37].

2.3. Synthesis of nanoparticles

AuNPs stabilized by citrate ions, with ca. 20 nm were synthesized by the Turkevich method [23], using 5.0 μmol HAuCl$_4$ in 19 mL of boiling water and 2 mL of 0.5% sodium citrate, prepared according to the procedure previously described [34,38].

2.4. Gold modification

Gold slides were immersed into a mixed solution containing 1 mM CS_2 and 50 μg/mL protein A in PBS for 2 h at 4 °C. In the experiments with nanoparticles the prepared aqueous suspension of AuNPs has been added to the former mixture to a final concentration of 4 nM, and left to incubate during 16 h at 4 °C. The concentrations used in this study were selected based on previous works [12,34,38]. As shown in Table S1 and Fig. S1 (in Supplementary material), ellipsometric and AFM data reveal that higher incubation time (16 h) was required to prepare nanostructured electrodes with high density of nanoparticles. After the modification, the substrates were abundantly rinsed with PBS and water. The concentrations of CS_2, protein A, AuNPs and the reaction time were kept constant in all the experiments.

2.5. Surface plasmon resonance

SPR measurements were carried out in a BIOSUPLAR400 T compact SPR sensor manufactured by "Analytical μ-Systems" coupled to a peristaltic pump from ISMATEC at a flow of 50 μL/min. After the modification, the gold slides were mounted onto the SPR equipment and 0.1 mg/mL IgG was pumped into the system and left to incubate for, approximately, 1 h. After PBST washing, a blocking step was performed with BB and, after a new PBST washing, 0.1 mg/mL anti-IgG was delivered into the cell. SPR experiments were conducted after a stable baseline was acquired. Data shown are the representative behavior of at least 3 independent experiments and are presented as absolute differences in resonance units (RU). The signal noise level was determined to be ≤1 RU. The IgG and anti-IgG concentrations were kept constant in all the experiments, unless noted otherwise.

2.6. UV–vis spectrophotometry

UV-vis spectrophotometry was performed using a UV-2600 spectrophotometer (Shimadzu), under the absorbance mode, over a scanning range from 200 to 800 nm with 2 nm intervals. The characterization was performed before and after the functionalization of the AuNPs with CS_2 and protein A, for 2 h in aqueous solution, under stirring.
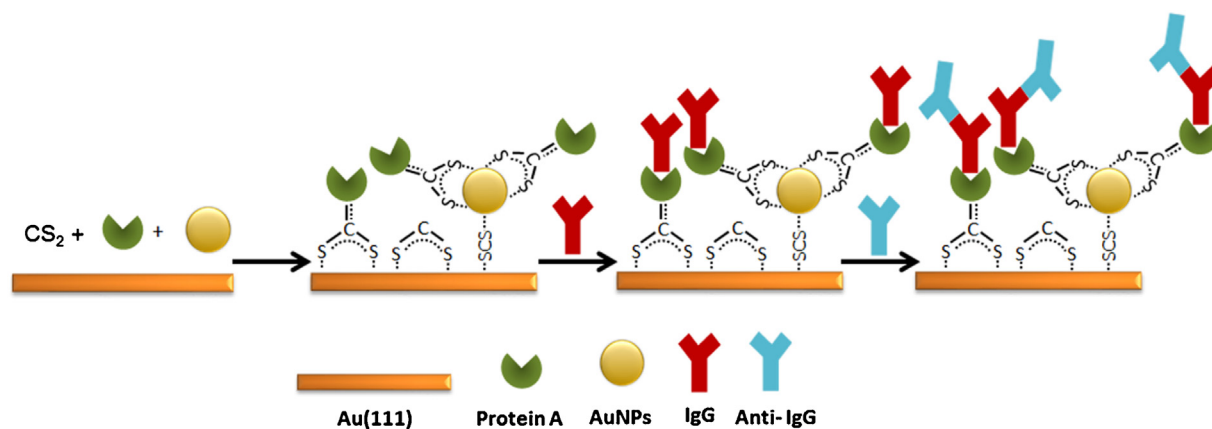
Fig. 1. Schematic diagram of the IgG immobilization strategy used in this work. AuNPs were mixed in the solution containing CS_2 and protein A to modify the gold surface and the performance of the immunosensor interface was evaluated directly through the biorecognition of anti-IgG. Given the spontaneity of the methodology it is expected that several sulfur species can interact with the gold surface, as proposed in the scheme. The representations are not to scale and, for simplicity, all the antibodies were represented with the same relative orientation. Due to the complex nature of the S-Au bonds, in particular in the adsorption of CS_2 and proposed Au-SCS-AuNPs entities, it was decided to use dotted lines to describe the linkages to the gold surfaces, in similarity with published work for other sulfur adsorbates [36].

2.7. Atomic force microscopy

AFM measurements were performed in air at $23 \pm 1\,°C$, using a Multimode Nanoscope IIIa microscope (Digital Instruments, Bruker) in tapping mode at a scan rate close to 1.6 Hz. For this purpose, etched silicon probes (TESP, with a resonance frequency close to 300 kHz, Bruker) were used. Au(111) modified substrates were imaged before and after incubation with 0.1 mg/mL IgG and 0.1 mg/mL anti-IgG for 1 h each. All images were obtained after thoroughly rinsing with PBS and water and drying under N_2 flow. A set of, at least, 3 independent experiments was performed for each system. Images of citrate stabilized-AuNPs, before and after modification with CS_2 and protein A in colloidal suspension, were acquired by placing a drop of the colloidal suspension onto freshly cleaved mica surface for 20 min, rinsing with water and drying with pure N_2.

2.8. Conventional ellipsometry

Ellipsometric measurements were performed in air at an incidence angle of 70° using a SE 400 Ellipsometer (Sentech Instruments) equipped with a He-Ne laser (632.8 nm). To obtain the optical parameters of the bare gold, a two-phase model was used and to estimate the thickness of the protein layer, a three-phase model was employed, as reported in the literature [12,39], fixing the real part of the refractive index at 1.5 [40]. The low extinction coefficient values (k) obtained in the measurements, except when AuNPs were attached to the surface, indicate the presence of nearly transparent films, as expected for thin organic layers [18]. The modified gold surfaces were incubated with 0.1 mg/mL IgG and anti-IgG in PBST for 1 h at room temperature. Before the measurements, they were rinsed with PBS and water.

2.9. Total internal reflection imaging ellipsometry

As previously described [41,42], the TIRIE system, which is based on an imaging ellipsometer under the total internal reflection mode, uses the evanescent wave to detect several physical, chemical and biochemical processes at the interfaces, as a real-time and label-free tool operating in a null and off null mode. A SF10 glass slide coated with a thin gold film (30 nm) is used as a substrate for TIRIE biosensing. A SF10 glass prism is tightly coupled to the glass side of the substrate, by an index matching oil, and the thin gold film side of the substrate contacts with the tested solutions through a microfluidic system, designed for microarray biosensor. The probe beam passes perpendicularly through a polarizer and a compensator (a quarter wave plate), into the glass prism and finally onto the gold film. When the incident angle is larger than the critical angle of total reflection, the beam is not transmitted through the gold film into the solution and a total internal reflection phenomenon occurs with the appearance of an evanescent field on the surface of the gold film. The deposition of protein layers on the gold surface alters the evanescent field, so that the polarized state of reflection is changed. In this case, the analysis of the polarized state of reflection will provide information about the amount of immobilized proteins on the biosensor surface. Moreover, the fact that the decay distance of evanescent field propagating into the layers on gold surface is about 100 nm, makes the solution concentration disturbance almost negligible on the image. The reflection beam passes through an analyzer and is focused by an imaging lens on a charge couple device (CCD) camera. A series of images with information on the subsequent protein layers interaction is then recorded by the TIRIE system. The reflection intensity is represented in grayscale and the changes in the grayscale value reflect the variations of mass surface concentration on the interface. A higher grayscale value implies a larger mass surface concentration. For the same protein layer, the grayscale value is nearly proportional to the mass surface concentration of the protein layer within the range of 0–10 nm [41]. Compared with the SPR technique, TIRIE not only acquires the light intensity information like SPR response, but also provides the ellipsometric phase sensitive results, leading to achieve higher sensitivity [43,44]. 0.1 mg/mL IgG and anti-IgG solutions in PBST and BB were injected *in situ*, during the experiment. Before and after measurements, the modified gold slides were rinsed with PBST and water to remove any weakly bounded molecules.

3. Results and discussion

3.1. Formation of DTC/AuNPs assemblies in colloidal suspension

Our methodology is based on the one-step gold substrate modification with a solution containing CS_2, protein A and AuNPs. In order to prove the biofunctionalization of the AuNPs, the reaction was followed first in solution, by UV–vis spectrophotometry (Fig. 2). The CS_2 aqueous solution presents a typical peak near 315 nm [12] and protein A at 280 nm, due to the presence of the phenylalanine and tyrosine residues in its structure [45]. AuNPs
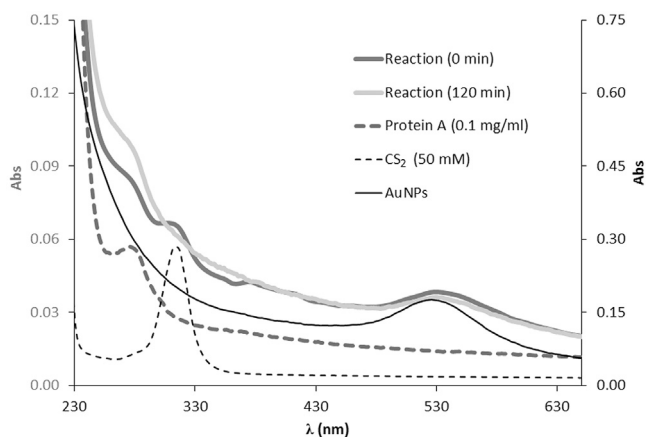
Fig. 2. UV–vis absorption spectra of AuNPs (ca. 20 nm), CS_2, protein A and of a mixture of protein A and CS_2 at 0 min and 120 min in aqueous solution. Grey line spectra should be read in the left yy axis and the black line spectra in the right yy axis.

colloidal suspension shows the typical SPR band around 530 nm, in agreement with the reported behavior for AuNPs stabilized by citrate ions with ca. 20 nm of diameter [23,33,34,46]. The two DTC absorption characteristic peaks appear at ca. 260 nm and 290 nm, depending on the nature of the amine groups involved in its formation [12,19,47]. Upon 2 h of incubation with CS_2 and protein A, the AuNPs absorption band at 530 nm exhibits a slight displacement to

higher wavelength, pointing to an increase in the average size of the AuNPs [33]. The appearance of a new absorption band between 260 and 290 nm can be assigned to the DTC formation by means of the several types of amine groups present in protein A that can react with CS_2. This reaction is corroborated by the consumption of CS_2 through the disappearance of its band at 315 nm. Overall, the results confirm the presence of protein A with DTC linkages as well as their interaction with nanostructured gold surfaces.

AFM imaging was used to characterize the morphology of AuNPs colloidal suspension before and after biofunctionalization with CS_2 and protein A (Fig. 3). Protein A from *Staphylococcus aureus* is a single-chain polypeptide with a Stokes Radius of 5 nm [48], and thus diameters between 30 and 40 nm should be expected for AuNPs with ca. 20 nm modified with 1 molecule and fully covered with Protein A, respectively. Fig. 3a presents an image of freshly synthesized AuNPs and a corresponding size histogram showing an average diameter of 21 ± 5 nm. Upon the reaction with CS_2 and protein A, the AuNPs tend to form small aggregates, clearly depicted in Fig. 3b and 3c, that were not visualized before and should be assigned to the presence of bionanoconjugates. Overall, a broader particle size distribution was obtained, shifted to larger diameters, with an average value of 31 ± 8 nm, clearly indicating the biofunctionalization with protein A. The smaller structures with ca. 16 nm of diameter might correspond to unmodified AuNPs or to small aggregates of protein A directly adsorbed to the mica surface.
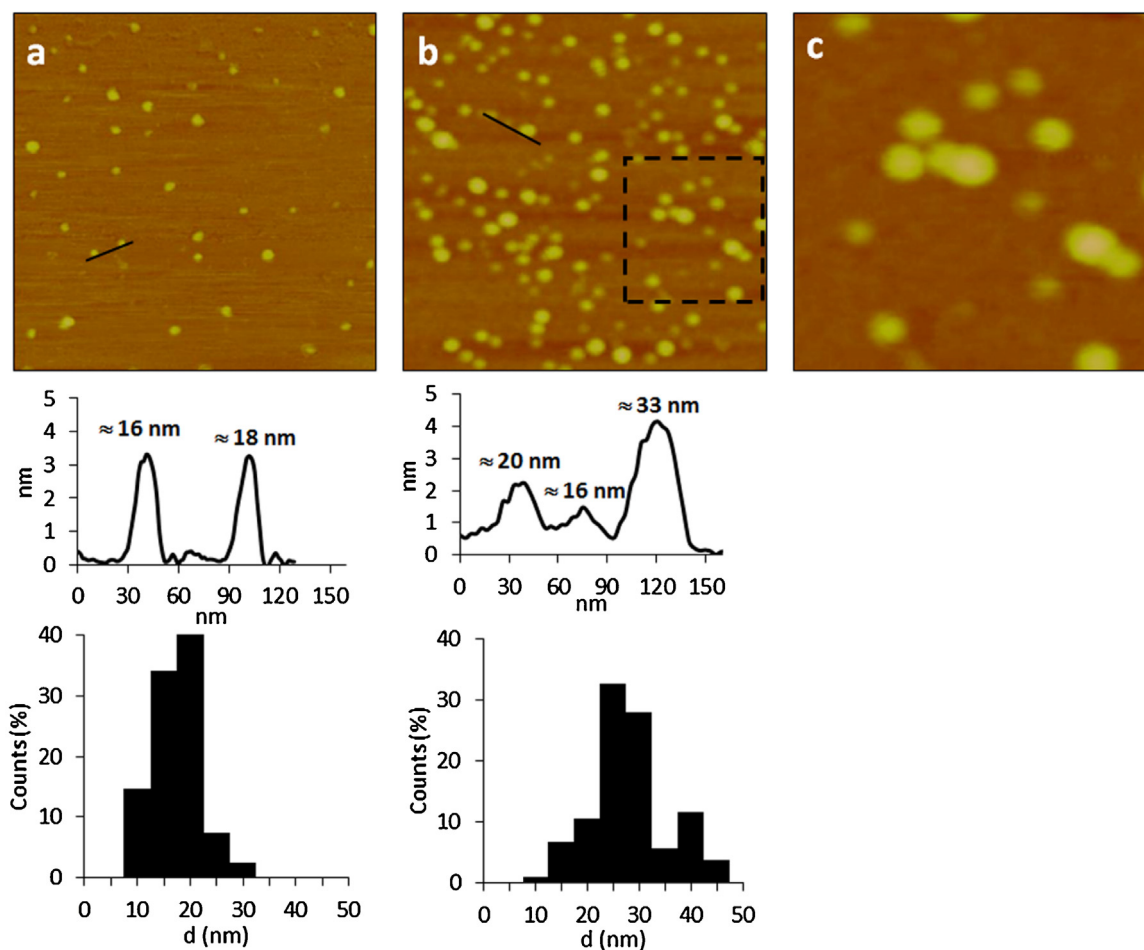

Fig. 3. AFM topographic images of mica after drop casting of AuNPs (a) before and (b) after reaction with CS_2 and protein A (750×750 nm^2, Z = 15 nm). The topographic profiles of representative areas are depicted below the corresponding topographic image, as well as the size distribution histograms. (c) Detail (300×300 nm^2, Z = 15 nm) of the topographic image presented in (b).
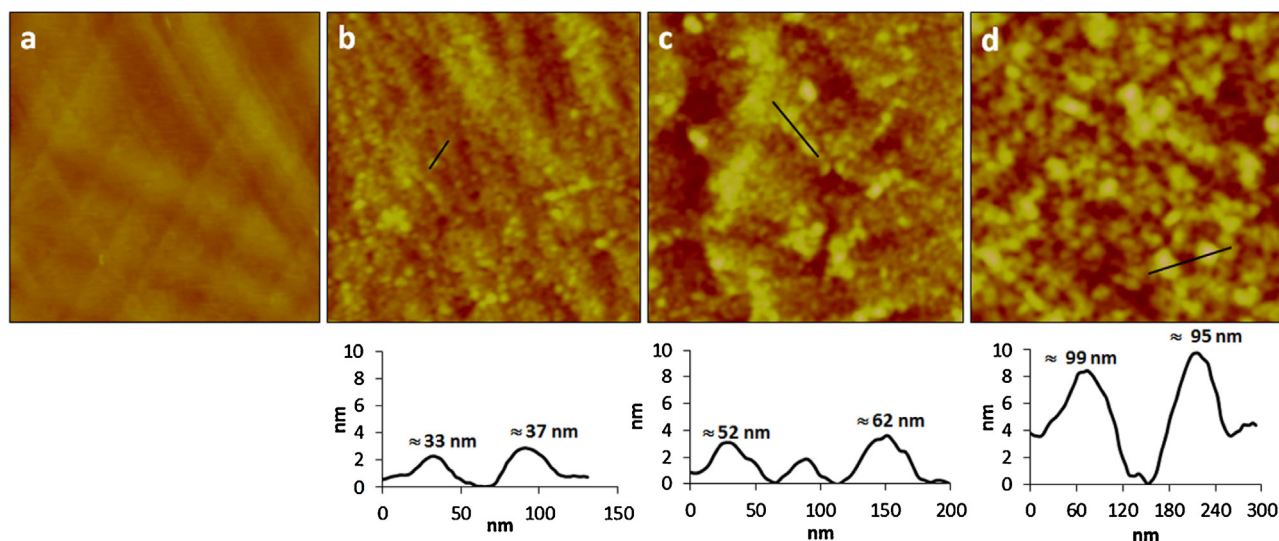
Fig. 4. AFM topographic images of (a) bare gold, (b) gold modified with CS_2, protein A and AuN*P*s, (c) after further immobilization of IgG and (d) posterior incubation with anti-IgG ($1 \times 1\,\mu m^2$, $Z = 15\,nm$). Below each topographic image, the topographic profiles of representative areas are depicted.

3.2. Optical and morphological characterization of the immunosensor assembling

Upon the modification of the gold substrate with a solution containing only CS_2 and protein A, an organic layer is readily formed with an estimated average optical thickness of 1.77 nm (Table 1), assuming a three-phase model [49,50] and a refractive index of 1.5 [40]. It can be seen that it is the ellipsometric parameter Δ that mostly contributes to the thickness change, since the parameter Ψ has only slightly changed after the surface modification. However, when AuNPs are also included in the deposition solution, the decrease in parameter Δ is accompanied by a significant change in parameter Ψ (*cf.* Table S1 and Fig. S1c, Supplementary Material), which can be attributed to the presence of the nanostructured gold on the substrate. In the absence of AuNPs, k values remain low (from 0.047 to 0.145), revealing that the organic films formed are nearly transparent, as expected for thin protein layers [18]. The addition of the AuNPs to the system make difficult the use of conventional ellipsometry at a fixed wavelength, since their optical properties are profoundly distinct from those of bulk gold surfaces [40]. In fact, several studies performed with films of AuNPs have pointed out that its nonmetallic optical and electronic properties [51,52], allied with the variation of its refractive index in the SPR region, preclude the use of conventional effective medium approaches based on averaging the optical properties of bulk materials [40]. Taking this into account and, as confirmed by the drastic variation in the Ψ value after the introduction of the AuNPs, the optical parameters (d_f and k) were not estimated for this step. However, after further incubation of the surface with both IgG and anti-IgG, the Ψ values become closer to those obtained in the absence of AuNPs and therefore the three-phase model may be again employed. Actually, after thickness estimation, the k values are close to 0, similarly to those obtained in the absence of AuNPs, revealing that the optical properties of the layers are mainly due to outer layers of the biological components, which are also expected to form nearly optically transparent layers.

The morphology of modified gold surfaces was characterized by AFM (Fig. 4). After incubation with CS_2, protein A and AuNPs (Fig. 4b), the gold surface shows small granular features that should correspond to protein A molecules adsorbed to the gold surface via CS_2. For comparison with modified interfaces, an image of a bare gold substrate is shown in Fig. 4a, exhibiting the preferred crystal-

lographic (111) orientation and displaying the typical triangularly shaped monoatomic terraces [37]. The larger globular structures are assigned to the modified AuNPs, as proposed in Fig. 1, where the sulfur moieties of CS_2 (or DTC) should be involved in the stable attachment of AuNPs to the gold surface. This type of linkage was previously supported by electrochemical reductive desorption studies and X-ray photoelectronic data analysis [34]. Moreover, to prove the crucial role of CS_2 interlinking AuNPs to gold, AFM images of Au(111) incubated with only AuNPs, or in presence of CS_2 were acquired (Fig. S1, Supplementary material). It is clearly evident that in the absence of CS_2 (Fig. S1 a), only residual AuNPs stay linked to the substrate after the washing step. In contrast, when CS_2 is added (Fig. S1 b and 1c, after 2 and 16 h, respectively), a significant amount of AuNPs is attached to the substrate. These results strongly indicate that the presence of the AuNPs in the immunosensing platform is due to the interaction of CS_2 with both the substrate and the AuNPs, which is conceivable due to the high strength of S-Au bonds, in the order of covalent linkage [53,54], instead of only a weak physical interaction. Also, the topography of the modified substrate with only CS_2 and protein A [12] is substantially different from Fig. 4a, where it is possible to distinguish small globules set apart and well distributed, assigned to protein A co-adsorbed with CS_2.

The modified gold surface was further incubated with IgG solution, resulting in an optical thickness increase to 6.71 nm in the presence of AuNPs, while in their absence the increase was only to 3.63 nm (Table 1). Since the thickness values obtained by conventional ellipsometry are correlated with the surface area covered by the protein molecules [55], IgG in this case, the higher thickness obtained when the AuNPs are incorporated in the system suggests, besides their successful immobilization, a higher amount of IgG adsorbed to the gold surface. Thus, the addition of the AuNPs to the solution used to modify the gold substrate enhanced the IgG specific immobilization on previously immobilized protein A at the surface. The presence of IgG molecules is clearly confirmed by AFM imaging and cross section (Fig. 4c), which reveals a high amount of larger globular structures than those assigned to the nanoconjugates depicted in Fig. 4b.

The capability of IgG to capture the anti-IgG was further evaluated by incubating the gold substrate containing the IgG, already immobilized, with an anti-IgG solution. Upon this step, the surface thickness increase was estimated in 5.6 nm in the presence of AuNPs and in only 3.3 nm without nanoparticles. Once more, the

Table 1
Ellipsometric parameters (ψ and Δ) of the IgG and anti-IgG immobilization on the modified gold surfaces. The thickness values (d_f) were estimated as described in the Experimental section. The thickness variation (Δd_f) was calculated after the incubation of both IgG and anti-IgG solutions for each modified surface. [a]Values reported in [12].

| Modified surfaces	Ψ (°)	Δ (°)	d_f (nm)	Δd_f (m)	k
Au[a]	43.76 ± 0.03	109.5 ± 0.1	–	–	
Au/CS$_2$/Protein A[a]	43.61 ± 0.01	107.58 ± 0.04	1.77 ± 0.07	–	0.145 ± 0.007
Au/CS$_2$/Protein A/IgG[a]	43.63 ± 0.01	105.68 ± 0.02	3.63 ± 0.09	1.9 ± 0.2	0.076 ± 0.003
Au/CS$_2$/Protein A/IgG/Anti-IgG[a]	43.66 ± 0.01	102.42 ± 0.07	6.9 ± 0.2	3.3 ± 0.3	0.047 ± 0.004
Au	43.69 ± 0.02	109.1 ± 0.2	–	–	
Au/CS$_2$/AuNPs/Protein A	43.1 ± 0.20	106.5 ± 0.4	–	–	–
Au/CS$_2$/AuNPs/Protein A/IgG	43.40 ± 0.04	103.6 ± 0.2	6.71 ± 0.07	–	0.122 ± 0.001
Au/CS$_2$/AuNPs/Protein A/IgG/Anti-IgG	43.46 ± 0.05	98.55 ± 0.05	12.32 ± 0.07	5.6 ± 0.1	0.081 ± 0.001
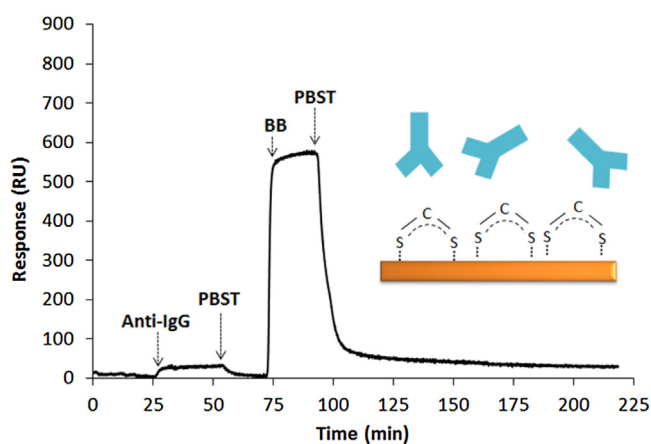
Fig. 5. Real-time SPR curve of a gold surface modified with only CS$_2$, showing the absence of interaction with anti-IgG and BB.

Table 2
Anti-IgG/IgG ratio by each modified gold surface. The values were calculated by the variations of the SPR data presented in Figs. 5 and 6.

Modified surfaces	Anti-IgG/IgG
Au/CS$_2$	–
Au/CS$_2$/Protein A	1.6
Au/CS$_2$/AuNPs/Protein A	2.1
Au/AuNPs/Protein A	0.8

substrate modified with AuNPs was able to capture a higher amount of anti-IgG than that prepared in the absence of AuNPs. The ellipsometric results are corroborated by the AFM image (Fig. 4d), since larger globular structures were formed due to the anti-IgG/IgG specific interaction. The presence of AuNPs, besides improving the surface coverage by protein A, allows to promote the IgG oriented immobilization by avoiding steric hindrance effects. Therefore, a proper IgG orientation results in an increase of the anti-IgG detection and then, high sensitivities can be achieved using this immunosensor platform.

3.3. Evaluation of the immunosensor performance

The ability of a gold substrate modified with only CS$_2$ to prevent nonspecific adsorption of anti-IgG was firstly tested, in real-time, by SPR, since it is known that IgG molecules extensively adsorb on bare gold surfaces [8]. In the absence of protein A and IgG, the adsorption of anti-IgG on gold with CS$_2$ is clearly inhibited (Fig. 5), since the SPR signal after a washing step with PBST has not changed. To further confirm the surface ability to inhibit protein nonspecific adsorption, a BB casein based solution was also injected into the cell and, after rinsing with PBST, the resulting optical signal increase is also negligible, meaning that almost no casein molecules adsorb to the surface. This confirms that CS$_2$ molecules are covering all the surface, establishing a strong interaction with gold, since in this case, the carbon atom loses its reactivity towards protein amine groups and does not form DTC linkages [13], preventing physical and chemical undesired adsorption.

IgG specific immobilization and further anti-IgG capture were also monitored through real-time SPR experiments as a way to test the immunosensor platform performance. As presented in the previous section, gold slides were modified, in one-step, with a mixed solution containing i) CS$_2$ and protein A, and ii) CS$_2$, protein A and AuNPs. Initially, both were injected with the IgG solution and later washed with PBST. In first case, the signal increase is 180 RU (Fig. 6a, grey curve), while in presence of AuNPs, it is 200 RU (Fig. 6a, black curve). This difference suggests that the presence of AuNPs results in the immobilization of higher amount of IgG, through the protein A, due to the larger amount of this latter bioreceptor, as firstly demonstrated by the ellipsometric results (Table 1).

After the addition of the anti-IgG solution, the SPR signal increase of the modified gold substrate containing AuNPs is 430 RU, while with the surface modified with only CS$_2$ and protein A the SPR signal rise is just 280 RU. By comparing both SPR responses and taking into consideration that anti-IgG does not adsorb nonspecifically to CS$_2$ modified surfaces, it is clear that the combination AuNPs/CS$_2$/protein A is responsible for the improvement of the IgG orientation and distribution at the surface, so that the steric constrains are low, enabling the specific detection of a larger amount of anti-IgG. This is proved by the higher anti-IgG/IgG ratio, that improves from 1.6 to 2.1 (Table 2), achieved in the absence and presence of AuNPs, respectively. Overall, using our strategy, a well-organized sensing surface can be assembled. IgG and anti-IgG were applied in our study as proof of concept, in order to mimic the natural and high specific antigen/antibody interaction. Using this pair of antibody/antigen, we were able to show that the developed immunosensing platform is efficient in detecting small amounts of target molecules, anti-IgG in the current illustrative approach.

When gold surfaces are modified with a mixed solution containing protein A and AuNPs, without CS$_2$ (Fig. 6b), the SPR signal increase is 364 and only 279, for IgG and anti-IgG respectively. This indicates that, in spite of a large amount of IgG is adsorbed on the surface, a much lower anti-IgG/IgG ratio (Table 2) is obtained for this sensing surface when compared to that attained in the presence of CS$_2$. Actually, in the absence of CS$_2$, the nonspecific adsorption is not prevented and thus the oriented immobilization of IgG cannot be ensured, since IgG molecules can adsorb to protein A and
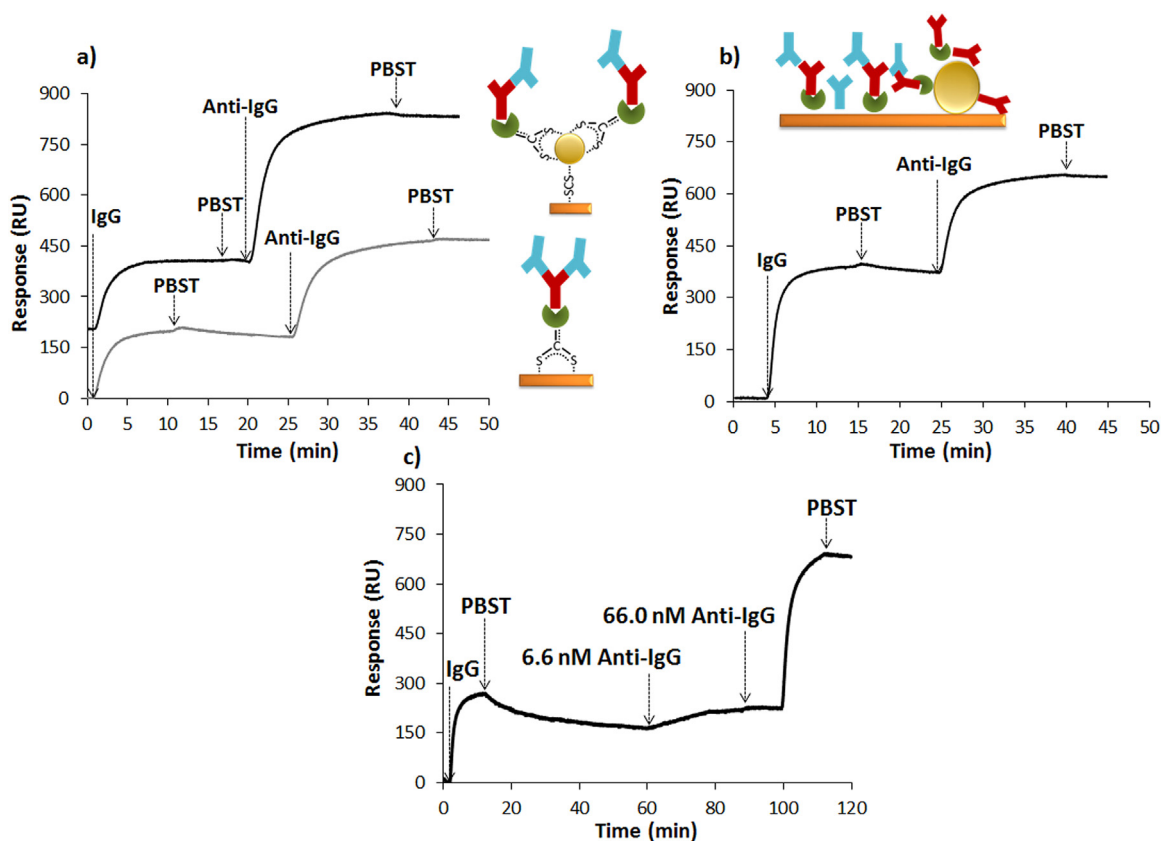
Fig. 6. Real-time SPR curves showing the interaction of IgG and anti-IgG with gold surface modified with (a) CS_2 and protein A (grey curve) and mixed with AuNPs (black curve) and (b) only protein A mixed with AuNPs. (c) Interaction of IgG and anti-IgG 6.6 nM and 66.0 mM with a gold surface modified with CS_2, protein A and AuNPs.

also directly to the gold surfaces (flat and nanoparticles). In this latter case, the specific biorecognition events should be reduced. Moreover, the unspecific adsorption of anti-IgG on unmodified gold cannot be excluded. These results clearly demonstrate the powerful combination of CS_2, protein A and AuNPs to prevent the undesired nonspecific adsorption of proteins and promote the proper orientation of the IgG molecules, without the need of external agents. The experiments were performed using IgG and anti-IgG 100.0 µg/mL, corresponding to a molar concentration of 660.0 nM. To assess the platform sensitivity, we reduced the antigen concentration to (6.6 nM) (Fig. 6c) and for such a small anti-IgG concentration, the platform maintains the capability to detect the anti-IgG specifically.

The performance assay of the developed interface was also conducted using TIRIE (Fig. 7). Compared to conventional ellipsometry, TIRIE biosensor is performed under the total internal reflection mode, hence observing the dynamic process of the biomolecules interaction. Its working principle, as explained in detail in the experimental section, is based on the specific interaction of target molecules with ligands on the surface (nonspecific adsorption must be avoided), which results in an increase of the surface density, quantitatively measured by density changes in grayscale values collected on a CCD camera. Thus, the grayscale reflects the dynamics of the biomolecular interactions over the time, similarly to SPR, but with higher sensitivity [43,44,56].

The modified gold substrate with CS_2, protein A and AuNPs was used as the sensing surface for the IgG immobilization and, for this step, a grayscale variation of 2680 is measured. Even after the washing step with PBST and the further injection with BB solution, the grayscale value remains unchanged, indicating a specific immobilization of IgG to the protein A molecules, as well as a blocking effect of the protein nonspecific adsorption. Finally, the anti-IgG detection was followed, and a variation of 8480 is detected in the grayscale
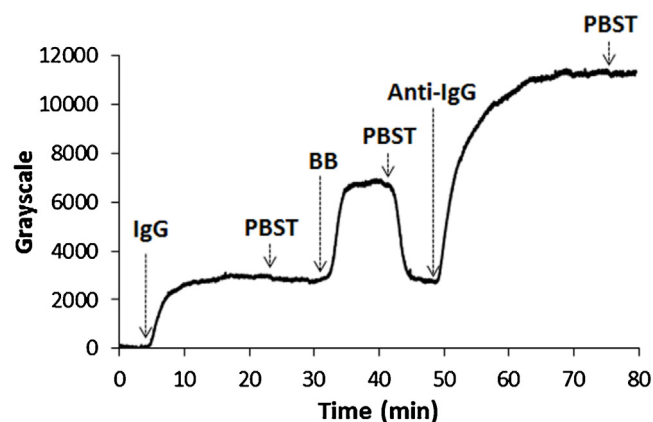

Fig. 7. Grayscale curve showing the interaction of IgG and anti-IgG with gold surface modified with CS_2 and protein A mixed with AuNPs.

value. This significant grayscale increase represents an anti-IgG/IgG ratio of 3.2, which corresponds to more than 2 anti-IgG molecules linked per each IgG, which is in agreement with the fact that the anti-IgG (secondary antibody) can react with several sites on the IgG (primary antibody) [18]. Furthermore, this evidence is corroborated by previous results obtained for covalently adsorbed IgG on SAM [8], proving that this is a proper platform to monitor the anti-IgG detection by properly oriented IgG and, therefore, to be used as an immunosensor.

4. Conclusions

In this work, we present a new surface modification approach, to be employed in the development of immunosensing platforms, based on the simple incubation of gold substrates with carbon disulfide, protein A and AuNPs. The functionalization of AuNPs with protein A, through the DTC formation, was confirmed by UV–vis spectrophotometry, whereas AFM imaging proved the overall size increase of AuNPs bioconjugates. By combining the surface characterization techniques, ellipsometry and AFM, we clearly demonstrated that flat gold surfaces can be functionalized with protein A nanostructures in only one-step. A proper orientation and distribution of IgG on the surface was revealed by the specific and sensitive detection of anti-IgG followed by real-time SPR. The CS_2 molecules that should co-adsorb together with bionanoconjugates during the one-pot reaction, explain the unique ability of this interface to block the protein nonspecific adsorption, as demonstrated also by SPR measurements. The addition of AuNPs to the gold surface modification reaction resulted in a higher anti-IgG/IgG ratio, than that obtained for gold modified with only CS_2 and protein A, revealing the potentiality of the platform to be employed in the immunosensors development. The immunosensing capability of the novel nanostructured interface was further validated by TIRIE, a high throughput optical technique for the detection of biomolecular interactions. Our one-step method to prepare the biorecognition layer, presents a simple and low-cost strategy to modify gold surfaces, avoiding the use of i) previous modification of the substrate, or the antibodies, or the nanoparticles, ii) extra steps requiring coupling agents for protein covalent linkage, and iii) blocking agents to inhibit the protein nonspecific adsorption. As proof of concept, we tested the platform performance by using the IgG/anti-IgG pair. However, it can be applied to any antibody/antigen detection, including those requiring competitive assays and/or sandwich configurations. Therefore, this versatile strategy presents high potential to be employed in the development of immunosensor interfaces.

Acknowledgements

Appendix A. Supplementary data

Supplementary data associated with this article can be found, in the online version, at http://dx.doi.org/10.1016/j.apsusc.2017.03.180.

References

[1] A. Ulman, Formation and structure of self-sssembled monolayers, Chem. Rev. 96 (1996) 1533–1554.
[2] J.C. Love, L.A. Estroff, J.K. Kriebel, R.G. Nuzzo, G.M. Whitesides, Self-assembled monolayers of thiolates on metals as a form of nanotechnology, Chem. Rev. 105 (2005) 1103–1170.
[3] J.B. Schlenoff, M. Li, H. Ly, Stability and self-exchange in alkanethiol monolayers, J. Am. Chem. Soc. 117 (1995) 12528–12536.
[4] R. Colorado, R.J. Villazana, T.R. Lee, Self-assembled monolayers on gold generated from aliphatic dithiocarboxylic acids, Langmuir 14 (1998) 6337–6340.
[5] M. Frasconi, F. Mazzei, T. Ferri, Protein immobilization at gold-thiol surfaces and potential for biosensing, Anal. Bioanal. Chem. 398 (2010) 1545–1564.
[6] K.L. Prime, G.M. Whitesides, Self-assembled organic monolayers: model systems for studying adsorption of proteins at surfaces, Science 252 (1991) 1164–1167.
[7] S. Flink, F.C.J.M. van Veggel, D.N. Reinhoudt, Sensor functionalities in self-assembled monolayers, Adv. Mater. 12 (2000) 1315–1328.
[8] Z.H. Wang, A.S. Viana, G. Jin, L.M. Abrantes, Immunosensor interface based on physical and chemical immunoglobulin G adsorption onto mixed self-assembled monolayers, Bioelectrochemistry 69 (2006) 180–186.
[9] X. Yang, Y. Guo, A. Wang, Luminol/antibody labeled gold nanoparticles for chemiluminescence immunoassay of carcinoembryonic antigen, Anal. Chim. Acta 666 (2010) 91–96.
[10] J.L. Acero Sanchez, A. Fragoso, H. Joda, G. Suarez, C.J. McNeil, C.K. O'Sullivan, Site-directed introduction of disulfide groups on antibodies for highly sensitive immunosensors, Anal. Bioanal. Chem. 408 (2016) 5337–5346.
[11] Y. Zhao, W. Pérez-Segarra, Q. Shi, A. Wei, Dithiocarbamate assembly on gold, J. Am. Chem. Soc. 127 (2005) 7328–7329.
[12] Y. Niu, A.I. Matos, L.M. Abrantes, A.S. Viana, G. Jin, Antibody oriented immobilization on gold using the reaction between carbon disulfide and amine groups and its application in immunosensing, Langmuir 28 (2012) 17718–17725.
[13] I. Almeida, A.C. Cascalheira, A.S. Viana, One step gold (bio)functionalisation based on CS2-amine reaction, Electrochim. Acta 55 (2010) 8686–8695.
[14] H. Zhu, D.M. Coleman, C.J. Dehen, I.M. Geisler, D. Zemlyanov, J. Chmielewski, G.J. Simpson, A. Wei, Assembly of dithiocarbamate-anchored monolayers on gold surfaces in aqueous solutions, Langmuir 24 (2008) 8660–8666.
[15] A.L. Eckermann, J.A. Shaw, T.J. Meade, Kinetic dispersion in redox-active dithiocarbamate monolayers, Langmuir 26 (2010) 2904–2913.
[16] P. Morf, F. Raimondi, H.-G. Nothofer, B. Schnyder, A. Yasuda, J.M. Wessels, T.A. Jung, Dithiocarbamates: functional and versatile linkers for the formation of self-assembled monolayers, Langmuir 22 (2006) 658–663.
[17] J.T. Marquês, R.F.M. de Almeida, A.S. Viana, Biomimetic membrane rafts stably supported on unmodified gold, Soft Matter 8 (2012) 2007–2016.
[18] I. Almeida, J.T. Marquês, W. Liu, Y. Niu, R.F.M. de Almeida, G. Jin, A.S. Viana, Phospholipid/cholesterol/decanethiol mixtures for direct assembly of immunosensing interfaces, Colloids Surf. B 136 (2015) 997–1003.
[19] K. Chen, H.D. Robinson, Robust dithiocarbamate-anchored amine functionalization of Au nanoparticles, J. Nanopart. Res. 13 (2011) 751–761.
[20] A.P. Leonov, A. Wei, Photolithography of dithiocarbamate-anchored monolayers and polymers on gold, J. Mater. Chem. 21 (2011) 4371–4376.
[21] I. Almeida, F. Henriques, M.D. Carvalho, A.S. Viana, Carbon disulfide mediated self-assembly of Laccase and iron oxide nanoparticles on gold surfaces for biosensing applications, J. Colloid Interface Sci. 485 (2017) 242–250.
[22] W.R. Glomm, Functionalized gold nanoparticles for applications in bionanotechnology, J. Disper. Sci. Technol. 26 (2005) 389–414.
[23] J. Kimling, M. Maier, B. Okenve, V. Kotaidis, H. Ballot, A. Plech, Turkevich method for gold nanoparticle synthesis revisited, J. Phys. Chem. B 110 (2006) 15700–15707.
[24] H. Li, B. Xu, D. Wang, Y. Zhou, H. Zhang, W. Xia, S. Xu, Y. Li, Immunosensor for trace penicillin G detection in milk based on supported bilayer lipid membrane modified with gold nanoparticles, J. Biotechnol. 203 (2015) 97–103.
[25] Y. Uludag, I.E. Tothill, Cancer biomarker detection in serum samples using surface plasmon resonance and quartz crystal microbalance sensors with nanoparticle signal amplification, Anal. Chem. 84 (2012) 5898–5904.
[26] Z. Jiang, Y. Qin, Z. Peng, S. Chen, S. Chen, C. Deng, J. Xiang, The simultaneous detection of free and total prostate antigen in serum samples with high sensitivity and specificity by using the dual-channel surface plasmon resonance, Biosens. Bioelectron. 62 (2014) 268–273.
[27] T.A. Taton, C.A. Mirkin, R.L. Letsinger, Scanometric DNA array detection with nanoparticle probes, Science 289 (2000) 1757–1760.
[28] L. He, E.A. Smith, M.J. Natan, C.D. Keating, The distance-dependence of colloidal Au-amplified surface plasmon resonance, J. Phys. Chem. B 108 (2004) 10973–10980.
[29] P. Englebienne, A.V. Hoonacker, M. Verhas, Surface plasmon resonance: principles, methods and applications in biomedical sciences, Spectroscopy 17 (2003) 255–273.
[30] A. de la Escosura-Muñiz, C. Parolo, A. Merkoçi, Immunosensing using nanoparticles, Mater. Today 13 (2010) 24–34.
[31] J.-W. Choi, D.-Y. Kang, Y.-H. Jang, J. Kim, B.-K. Oh, Ultra-sensitive surface plasmon resonance based immunosensor for prostate-specific antigen using gold nanoparticle-antibody complex, Colloids Surf. A 313–314 (2008) 655–659.
[32] P. Damborský, N. Madaboosi, V. Chu, J.P. Conde, J. Katrlík, Surface plasmon resonance application in prostate cancer biomarker research, Chem. Pap. 143 (2015).
[33] I. Almeida, S.G. Mendo, M.D. Carvalho, J.P. Correia, A.S. Viana, Catalytic Co and Fe porphyrin/Fe3O4 nanoparticles assembled on gold by carbon disulfide, Electrochim. Acta 188 (2016) 1–12.
[34] I. Almeida, V.C. Ferreira, M.F. Montemor, L.M. Abrantes, A.S. Viana, One-pot approach to modify nanostructured gold surfaces through in situ dithiocarbamate linkages, Electrochim. Acta 83 (2012) 311–320.
[35] Z. Wang, G. Jin, Feasibility of protein A for the oriented immobilization of immunoglobulin on silicon surface for a biosensor with imaging ellipsometry, J. Biochem. Biophys. Methods 57 (2003) 203–211.

[36] C.-A. Fustina, A.-S. Duwez, Dithioesters and trithiocarbonates monolayers on gold, J. Electron. Spectrosc. Relat. Phenom. 172 (2009) 104–106.

[37] J.T. Marquês, R.F.M. de Almeida, A.S. Viana, Lipid bilayers supported on bare and modified gold −Formation, characterization and relevance of lipid rafts, Electrochim. Acta 126 (2014) 139–150.

[38] V.C. Ferreira, A.F. Silva, L.M. Abrantes, Electrochemical and morphological characterization of new architectures containing self-assembled monolayers and Au-NPs, J. Phys. Chem. C 114 (2010) 7710–7716.

[39] H. Arwin, Spectroscopic ellipsometry and biology: recent developments and challenges, Thin Solid Films 313-314 (1998) 764–774.

[40] H.L. Zhang, S.D. Evans, J.R. Henderson, Spectroscopic ellipsometric evaluation of gold nanoparticle thin films fabricated using layer-by-layer self-assembly, Adv. Mater. 15 (2003) 531–534.

[41] Y.-Y. Chen, Z.-H. Wang, Y.-H. Meng, G. Jin, Biosensor with total internal reflection imaging ellipsometry, Int. J. Nanotechnol. 4 (2007) 171–178.

[42] G. Jin, Y.H. Meng, L. Liu, Y. Niu, S. Chen, Q. Cai, T.J. Jiang, Development of biosensor based on imaging ellipsometry and biomedical applications, Thin Solid Films 519 (2011) 2750–2757.

[43] I. Baleviciute, Z. Balevicius, A. Makaraviciute, A. Ramanaviciene, A. Ramanavicius, Study of antibody/antigen binding kinetics by total internal reflection ellipsometry, Biosens. Bioelectron. 39 (2013) 170–176.

[44] A.V. Nabok, A. Tsargorodskaya, A.K. Hassan, N.F. Starodub, Total internal reflection ellipsometry and SPR detection of low molecular weight environmental toxins, Appl. Surf. Sci. 246 (2005) 381–386.

[45] C.N. Pace, F. Vajdos, L. Fee, G. Grimsley, T. Gray, How to measure and predict the molar absorption coefficient of a protein, Protein Sci. 4 (1995) 2411–2423.

[46] W. Haiss, N.T. Thanh, J. Aveyard, D.G. Fernig, Determination of size and concentration of gold nanoparticles from UV-vis spectra, Anal. Chem. 79 (2007) 4215–4221.

[47] Y. Zhang, A.M. Schnoes, A.R. Clapp, Dithiocarbamates as capping ligands for water-soluble quantum dots, ACS Appl. Mater. Interfaces 2 (2010) 3384–3395.

[48] I. Björk, B.-Å. Petersson, J. Sjöquist, Some physicochemical properties of protein a from staphylococcus aureus, Eur. J. Biochem. 29 (1972) 579–584.

[49] J.T. Marquês, A.S. Viana, R.F.M. de Almeida, A biomimetic platform to study the interactions of bioelectroactive molecules with lipid nanodomains, Langmuir 30 (2014) 12627–12637.

[50] A.S. Viana, M. Kalaji, L.M. Abrantes, Self-assembled monolayers of Vitamin B_{12} disulphide derivatives on gold, Electrochim. Acta 47 (2002) 1587–1594.

[51] M. Brust, D. Bethell, C.J. Kiely, D.J. Schiffrin, Self-assembled gold nanoparticle thin films with nonmetallic optical and electronic properties, Langmuir 14 (1998) 5425–5429.

[52] T. Baum, D. Bethell, M. Brust, D.J. Schiffrin, Electrochemical charge injection into immobilized nanosized gold particle ensembles: potential modulated transmission and reflectance spectroscopy, Langmuir 15 (1999) 866–871.

[53] H. Häkkinen, The gold-sulfur interface at the nanoscale, Nat. Chem. 4 (2012) 443–455.

[54] E. Pensa, E. Cortés, G. Corthey, P. Carro, C. Vericat, M.H. Fonticelli, G. Benítez, A.A. Rubert, R.C. Salvarezza, The chemistry of the sulfur-gold interface: in search of a unified model, Acc. Chem. Res. 45 (2012) 1183–1192.

[55] H. Elwing, Protein absorption and ellipsometry in biomaterial research, Biomaterials 19 (1998) 397–406.

[56] L. Liu, Y.-y. Chen, Y.-h. Meng, S. Chen, G. Jin, Improvement for sensitivity of biosensor with total internal reflection imaging ellipsometry (TIRIE), Thin Solid Films 519 (2011) 2758–2762.